

Experimental study on demountable steel-concrete connectors subjected to combined shear and tension

Ee Loon Tan^{a,*}, Harshard Varsani^a, Feiyu Liao^b

^a School of Computing, Engineering and Mathematics, Western Sydney University, Australia

^b School of Transportation and Civil Engineering, Fujian Agriculture and Forestry University, China

ABSTRACT

Composite beams are being used increasingly in construction due to their benefits over beams consisting of the steel component alone. In some applications such as in composite coupling beams and infill walls, steel-concrete connectors must resist uplift forces in addition to shear forces. Therefore, there is a need to carry out experimental testing to investigate the performance of steel-concrete connectors under combined loading. Furthermore, the separation of the steel and concrete components is a destructive activity and requires remelting of the steel component if it is to be reused. Remelting requires energy that usually comes from unsustainable resources. Hence, research has been carried out in this paper on demountable steel-concrete connectors as they allow demounting and easy separation of the steel and concrete components and reuse.

The performance of three types of steel-concrete connectors subjected to combined shear and tensile loading was investigated experimentally. A pull-out test was carried out to determine the tensile resistance of each type of steel-concrete connector. This was followed by a series of modified push tests to determine the interaction between shear and tension loading. Tensile resistance which had been determined from pull-out tests was applied in increments of 25% to each group followed by shear loading until failure of the steel-concrete connector was observed.

Based on the experimental investigation carried out, significant reduction in shear resistance was observed when tension was applied. The results are also compared with existing relationships for headed studs under combined shear and tensile loading to determine which relationship is most reliable in predicting the shear-tension resistance interaction of demountable steel-concrete connectors.

1. Introduction

Composite beams are increasingly being used in construction due to their ability to withstand higher loads than if the beams are to be made by only one of its constituents. Headed studs are used in these types of beams to provide resistance to shear at the steel concrete interface. Significant research [4–12] has been carried out on the performance of headed studs under static and fatigue loading. This increasing usage of composite construction has led to use cases in which the steel-concrete connectors must resist both shear and tensile forces. Some examples of such use cases include composite coupling beams, truss bridges with connections between concrete slabs and diagonal members, infill walls and composite column bases. Therefore, research [13–16] has been carried out to determine the effects of combined loading on headed studs and varying relationships have been proposed to estimate the relationship between shear and tensile resistance of headed studs.

However, the traditional headed studs have a few disadvantages such as the requirement of a separate contractor to install the headed studs by welding to the steel section which subsequently requires quality assurance testing. Additionally, the structure must be demolished, and the steel section remelted so that it can be recycled to form

new steel sections. Remelting of the steel section requires significant quantities of energy which is a concerning matter seeing the increasing awareness of global warming and sustainability. To overcome this issue, researchers have experimented [17–22] with using demountable steel-concrete connectors to provide the shear resistance in composite beams. Some have repurposed blind bolts as steel-concrete connectors whereas some have milled threads onto the traditional headed stud to allow demounting. They are easy to install on site and allow deconstruction of the composite beam when the structure reaches its end of service life.

The experimental research conducted on demountable steel-concrete connectors has involved monotonic or fatigue shear loading. However, due to some use cases likely to subject tensile forces on the steel-concrete connectors, there is a need to carry out experimental investigation to determine if shear resistance is affected in the presence of tensile forces. Hence, an experimental study has been carried out on three type of demountable steel-concrete connectors under combined shear and tensile loading. The experimental program consisted of three pull-out tests, three standard push tests and nine modified push tests. Varying percentages of tensile force were applied to the modified push test to determine its effect on the shear resistance.

* Corresponding author.

E-mail addresses: e.tan@westernsydney.edu.au (E.L. Tan), 17597106@student.westernsydney.edu.au (H. Varsani), feiyu.liao@fafu.edu.cn (F. Liao).

Nomenclature

A_{no}	planner area of the concrete failure cone
d_{bs}, d_o, d_s	steel-concrete connector shank diameter
d_u	head diameter of the steel-concrete connector
E	Youngs modulus of material
f_c'	concrete cylinder compressive strength
f_{uf}, f_{uc}	ultimate yield stress of steel-concrete connector material
h_{ef}	effective embedment depth of the steel-concrete connector
h_{sc}	overall nominal height of steel-concrete connector
i	ductility index
k_{cp}	coefficient for pryout strength
K_{si}	shear stiffness
T	tension applied per steel-concrete connector
T_{cu}	initial tension applied for specimen under combined loading
T_u	maximum tension resistance

T_{u1}	ultimate tensile resistance of demountable headed studs
T_{u2}	ultimate tensile resistance of AJAX ONESIDE bolts
T_{u3}	ultimate tensile resistance of Hollo-Bolts
V	shear force applied per steel-concrete connector
V_{cu}	maximum shear resistance under combined loading
V_u	maximum shear resistance
$\Delta_{0.85}$	slip at 85% of maximum shear load on the post-peak descending branch
Δ_{max}, Δ_u	slip at maximum load
Δ_y	slip at yield point
λ	modification factor to account for the reduced mechanical properties of light weight concrete
σ_y	yield stress of material
σ_u	ultimate stress of material
ϵ_u	ultimate strain
$\psi_{c,N}$	modification factor to account for presence or absence of cracks when determining tensile resistance

2. Relationships proposed for the interaction in existing research

McMackin et al. [23] and cited by Saari et al. [13] experimented on headed steel anchors under combined shear and tensile loading and proposed an elliptical relationship, Eq. (1), based on their test results. However, this relationship requires the interaction to be considered in the design process regardless of the magnitude of the minor force. Alternatively, the tri-linear relationship, Eq. (2), proposed by Bode et al. [24,25] and adopted by both ACI 318-14 [26] and PCI 6th [27] requires the interaction to be considered only if the design shear or tensile force is greater than 20% of the ultimate shear or tensile strength of the steel-concrete connector. On the other hand, the translated circular relationship, Eq. (3), proposed by Lin et al. [14] allows for the interaction to be ignored if the design tensile or shear force is less than 10% of the tensile or shear resistance of the steel-concrete connector. Mirza et al. [15] developed a finite element model to investigate the behaviour of shear studs under combined shear and tensile loading for both solid and profiled slabs. This model was verified against experimental results and Eq. (4) was proposed to predict the interaction strength of headed studs under combined shear and tensile loading for profiled slab.

$$\left(\frac{V}{V_u}\right)^{5/3} + \left(\frac{T}{T_u}\right)^{5/3} \leq 1 \quad (1)$$

$$\frac{V}{V_u} + \frac{T}{T_u} \leq 1.2 \quad \text{if } V \geq 0.2V_u \quad \text{or} \quad T \geq 0.2T_u \quad (2)$$

$$\left(\frac{V}{V_u} + \frac{1}{2}\right)^2 + \left(\frac{T}{T_u} + \frac{1}{2}\right)^2 \leq 2.61 \quad \text{if } V \geq 0.1V_u \quad \text{or} \quad T \geq 0.1T_u \quad (3)$$

$$\left(\frac{V}{V_u}\right)^{3/2} + \left(\frac{T}{T_u}\right)^{3/2} = 1 \quad (4)$$

The test results of the experimental program are compared against these relationships to determine whether the same relationships can be used to predict the combined shear and tensile resistance of demountable steel-concrete connectors. A new relationship will be proposed where the existing relationships did not predict the strength within an acceptable margin.

3. Experimental study**3.1. Test specimens**

There were a total of fifteen test specimens equally divided in five groups. Each specimen was identified by the letter S, A or H for headed studs, AJAX ONESIDE and Hollo-Bolts respectively. This was followed

by a numerical value indicating the group that the specimen belonged to. The purpose of specimens in Group 1 was to determine the tensile resistance, Group 2 to determine the shear resistance and Group 3–5 to determine the shear-tension interaction resistance. The specimen summary is given in Table 1 below. In general, there were two distinct test specimens, one for the pull-out test and one for both push tests and modified push tests. Push tests were of the standard type, where a steel section with two concrete blocks connected with steel-concrete connectors is vertically loaded. Modified push tests were like the standard push test except that there were two additional hydraulic jacks between the two concrete blocks applying a lateral force (Applying a tensile force on the steel-concrete connectors). To summarise the specimen differences, tension resistance was determined from Group 1, shear resistance from Group 2 and interaction resistance from Group 3–5. Group 3–5 specimens had an initial fraction of their respective T_{u1} , T_{u2} or T_{u3} applied before shear load was applied until failure.

3.1.1. Push test and modified push test

Three push tests and nine modified push tests were carried out. Details of the push test specimens are shown in Fig. 1. Each specimen consisted of two $600 \times 600 \times 150$ mm concrete blocks with each

Table 1
Test specimen summary.

Group	Test specimen ID	Connector type	Initial tension applied	Shear force applied
Group 1	S1	Threaded headed stud	Until failure	No
	A1	AJAX ONESIDE	Until failure	No
	H1	Hollo-Bolt	Until failure	No
Group 2	S2	Threaded headed stud	No	Until failure
	A2	AJAX ONESIDE	No	Until failure
	H2	Hollo-Bolt	No	Until failure
Group 3	S3	Threaded headed stud	25% of T_{u1}	Until failure
	A3	AJAX ONESIDE	25% of T_{u2}	Until failure
	H3	Hollo-Bolt	25% of T_{u3}	Until failure
Group 4	S4	Threaded headed stud	50% of T_{u1}	Until failure
	A4	AJAX ONESIDE	50% of T_{u2}	Until failure
	H4	Hollo-Bolt	50% of T_{u3}	Until failure
Group 5	S5	Threaded headed stud	75% of T_{u1}	Until failure
	A5	AJAX ONESIDE	75% of T_{u2}	Until failure
	H5	Hollo-Bolt	75% of T_{u3}	Until failure

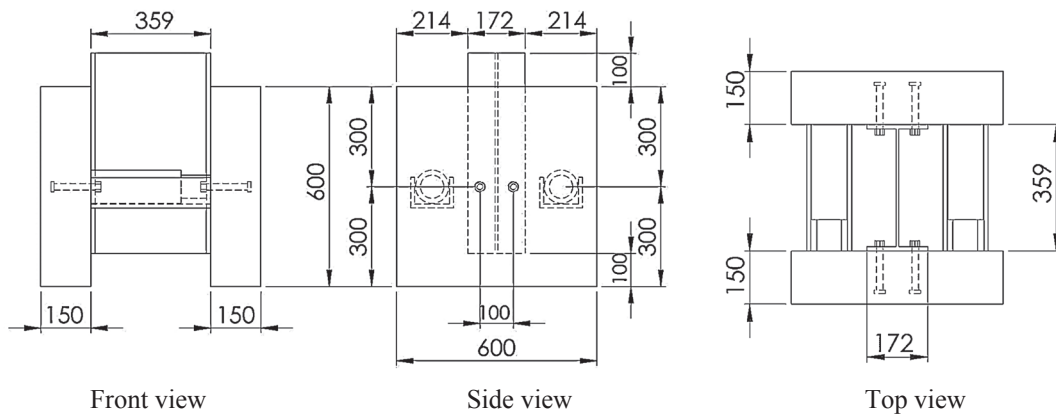


Fig. 1. Details of modified push test specimen (All dimensions in mm).

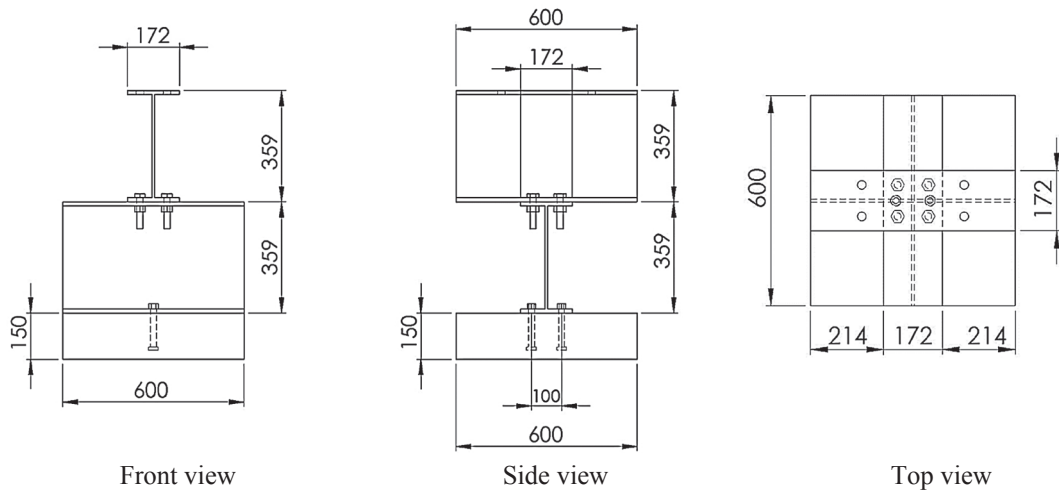


Fig. 2. Details of pull-out test specimen (All dimensions in mm).

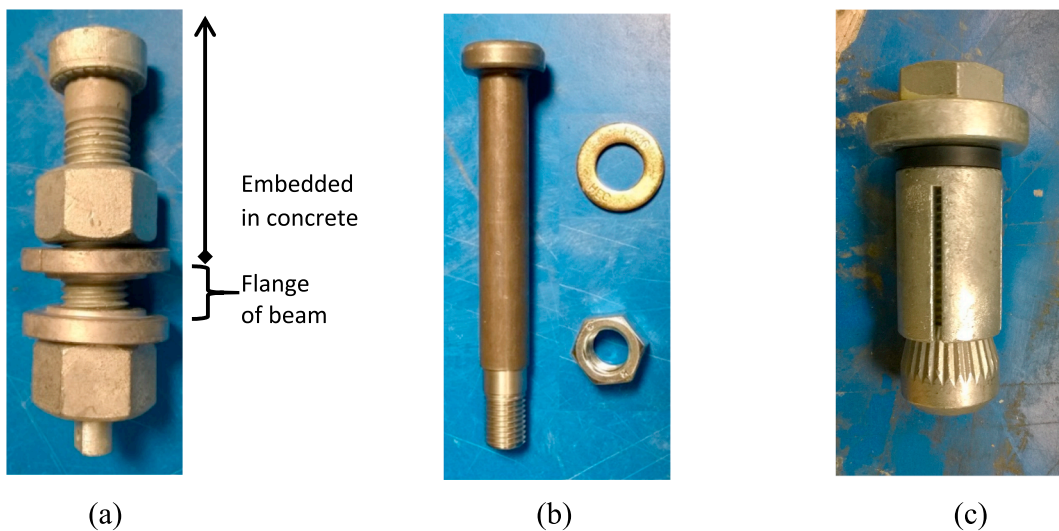


Fig. 3. Steel-concrete connector types, (a) AJAX ONESIDE; (b) Threaded headed stud; (c) Lindapter Hollo-Bolt.

concrete block having two steel-concrete connectors embedded in it and bolted to a 600 mm long steel section (360UB56.7) through pre-drilled holes. The diameter of the holes would be the same as the diameter of the steel-concrete connectors used. The size of steel section allowed the smaller tension jacks and their load cells to fit between the two concrete blocks. Both concrete blocks were reinforced with an

upper and lower mesh layer of 540 mm long N12 reinforcing bars spaced at 180 mm with a cover of 30 mm provided for both layers. The concrete blocks were casted horizontally from the same concrete mix to avoid variations in concrete strength. The concrete blocks were air cured for 28 days at which point the two halves of the steel beam were welded together to get the final specimen arrangement.

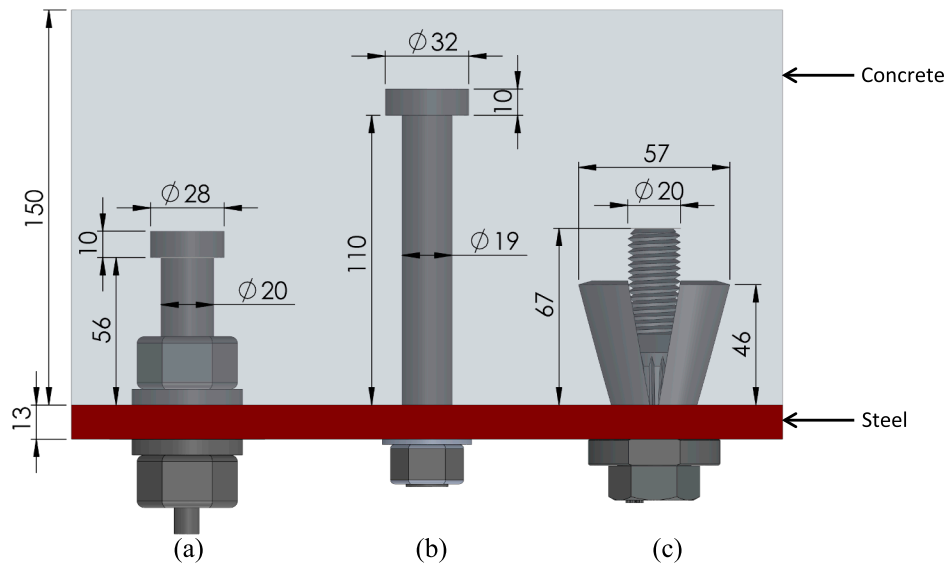


Fig. 4. Steel-concrete connectors' dimensions, (a) AJAX ONESIDE; (b) Demountable headed stud; (c) Lindapter Hollo-Bolt (All dimensions in mm).

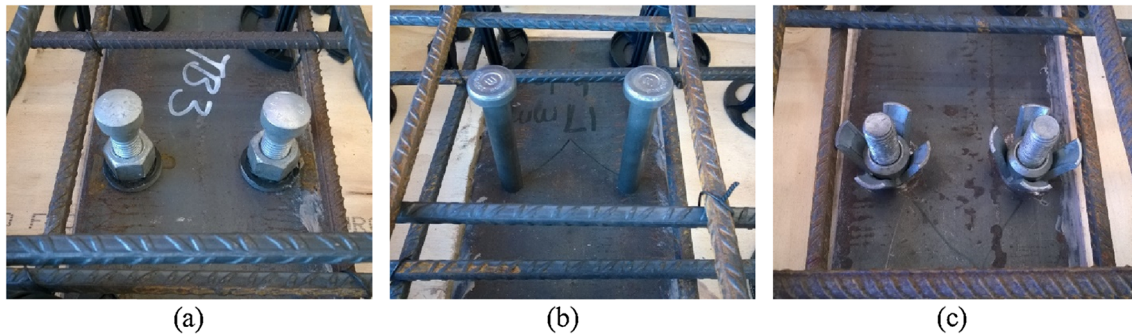


Fig. 5. Steel-concrete connectors after installation, (a) AJAX ONESIDE; (b) Threaded headed stud; (c) Lindapter Hollo-Bolt.



Fig. 6. Push test setup.

3.1.2. Pull-out test

To determine the tensile resistance, a pull-out test was carried out for each of the three types of steel-concrete connectors. The test specimen is depicted in Fig. 2. The specimen consists of two 360UB56.7 beams perpendicularly placed on top of each other and connected by four M20 bolts. Two steel-concrete connectors spaced 100 mm centre to centre are embedded in the concrete block through predrilled holes in the bottom beam. The primary purpose of the top beam was to increase the vertical height since the jack had a limited stroke length.

3.2. Installation of steel-concrete connectors

Three types of steel-concrete connectors tested in this experimental program are shown in Fig. 3 below and their respective dimensions are shown in Fig. 4 below. An additional nut was used when installing the AJAX ONESIDE in such a way that would allow clamping to the flange as well as provide a relatively higher tensile resistance. A torque wrench was used to tighten the AJAX ONESIDE to the manufacturer specified of 380 Nm. The second type of steel-concrete connector, 150 mm long demountable headed stud, was put through a milling process so that it could be made demountable. A 17 mm diameter and 13 mm long collar provided a ridge that prevented the headed stud from falling through the pre-drilled hole in the steel section. A further 17 mm long section was milled to accept an M16 nut and washer for fastening. The third and final type, Lindapter Hollo-Bolt, was installed using the standard installation procedure with a tightening torque of

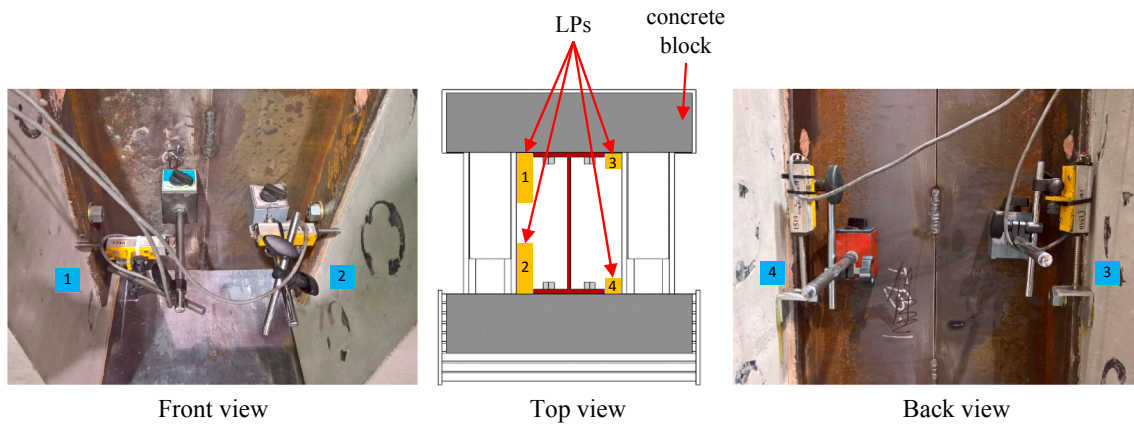


Fig. 7. Position of LPs for modified push tests.

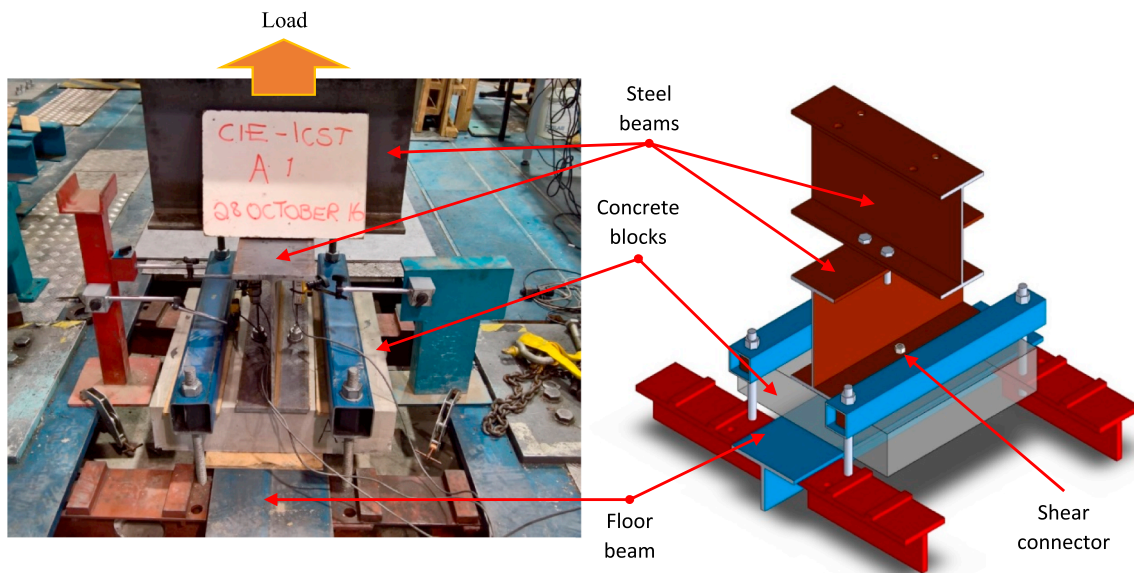


Fig. 8. Pull-out test set-up.

300Nm as specified by the manufacturer. All three demountable steel-concrete connectors after installation and before concrete casting are shown in Fig. 5.

3.3. Test setup, loading procedure and instrumentation

3.3.1. Push test

The test setup to determine the shear resistance is shown in Fig. 6. One of the concrete blocks was roller supported while the other had a fixed support. The purpose of the roller support was to make the resistance to horizontal movement of the concrete blocks negligible.

Displacement controlled load was applied at a rate of 0.016 mm/s by a 1000 kN resistance jack installed vertically until failure of the specimens was observed i.e. load dropped by approximately 20%. A thick metal plate was placed between the steel beam and the jack to ensure that the force was distributed evenly. Each specimen had two linear potentiometers (LP's) recording the lateral displacement of the concrete blocks (One LP per concrete block) and two LPs measuring the vertical slip of each specimen (One LP per concrete block). The relative positions of the LPs are shown in Fig. 7. Readings from the LPs and the load cell for the hydraulic jack were recorded by a data logger.

3.3.2. Pull-out test

The test setup of pull-out tests is shown in Fig. 8. The specimen was clamped to the floor beams by two square sections and the top beam was bolted using four M20 bolts to the jack's fully extended piston. During loading, the jack piston was retracted at a displacement-controlled rate of 0.016 mm/s thereby exerting a tensile force on the steel-concrete connectors. Loading continued until a sudden drop in load of at least 20% was observed. A LP measured the vertical displacement of each steel-concrete connector with respect to the floor beams. The readings from the load cell of the hydraulic jack and both LPs were recorded by a data logger.

3.3.3. Modified push test

The set-up for the modified push tests is shown in Fig. 9 (Reinforcement has been omitted for simplification purposes). Specimens were placed upright supported by rollers on one concrete block and a metal plate for the other concrete block. One jack was placed on each side of the web at the same elevation as the steel-concrete connectors to avoid eccentricity of tensile loading. Furthermore, the tension jacks were of the same type and were connected to a single manual hydraulic pump to ensure equal force was applied by each jack.

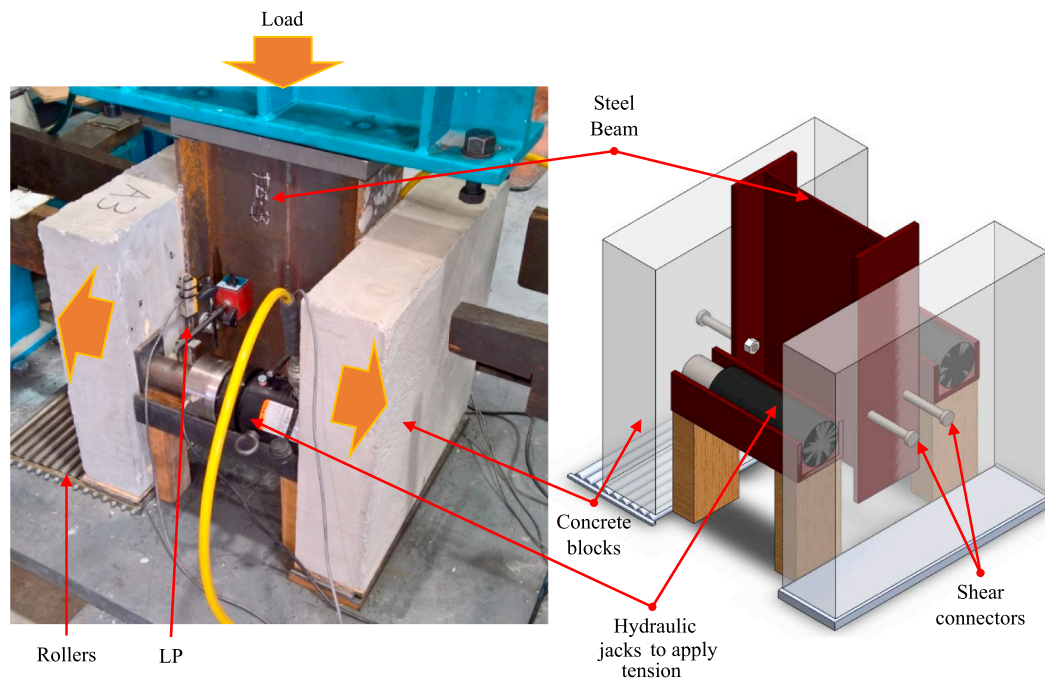


Fig. 9. Modified push test set-up.

Table 2
Concrete material properties test results.

	Average (MPa)	Standard deviation
7 day f_c' test	23.2	0.62
14 day f_c' test	27.2	1.07
21 day f_c' test	28.7	1.07
28 day f_c' test	30.1	1.50
Elastic modulus	34,667	1829
Static chord modulus	34,876	1660
Modulus of rupture	3.69	0.48

Table 3
Material properties of the steel-concrete connectors and steel section.

	E (GPa)	σ_y (MPa)	σ_u (MPa)
Steel section - flange	226	265	485
Steel section - web	219	330	500
Headed stud	206	338	553
AJAX ONESIDE	225	830	1018
Hollo-bolt	216	740	969

Type 2 loading was adopted for the modified push tests. This is whereby an initial tension force is applied by the two horizontal jacks followed by shear force until failure is observed i.e. sudden drop in shear load or the inability to maintain the tension at the required magnitude due to significant lateral separation of concrete blocks. The tensile force applied was 25, 50 and 75% of the ultimate tensile strength determined from pull-out tests of that respective steel-concrete connector type. When carrying out push tests, the concrete blocks naturally tend to separate laterally upon shear loading which leads to a reduction in the tensile force being resisted by the steel-concrete connectors. It was therefore decided to continuously monitor the tension jack load cell readings and adding pressure to the jacks to keep the tension within 1kN of the required magnitude. The position of LPs that measured the slip and lateral separation was identical to the push test shown in Fig. 7.

3.4. Material properties

To determine the concrete strength parameter, f_c' , 100 mm diameter by 200 mm long concrete cylinders were prepared for compression tests and tested at 7-day intervals up to 28 days. Three cylinders were tested at each of the 7-day intervals and their results averaged. Testing of the test specimens was carried out within a week after the 28-day curing period. Three more cylinders of the same size were tested on 28-day to determine the static chord modulus and the elastic modulus. Three beams 100 × 100 × 300 mm were also prepared from the concrete mix which were then tested in a modulus of rupture (MOR) test rig to determine the MOR of the concrete on day 28. The results of these three concrete material tests are shown in Table 2 below. Standard Deviation is calculated to determine the variation in test results between the three test samples for each material property test. The compressive strength test was carried out as per AS1012.9 [28], static chord modulus as per AS1012.17 [29] and modulus of rupture as per AS1012.11 [30]. Coupon tests were carried out to determine the material properties of the steel section and the three types of steel-concrete connectors tested. The results of these tests are given in Table 3.

4. Results and discussion

4.1. Load – Slip behaviour and ductility

4.1.1. Push test and modified push test

The load-slip curves of push test specimens are shown in Fig. 10 below. Applying 25% of the tensile resistance had a minimal effect on the load-slip behaviour of all three steel-concrete connectors compared to pure shear loading. However, significant difference in load-slip behaviour was observed when the initial tension applied was increased to 50% of the respective steel-concrete connectors' T_u . A considerable reduction in slip at failure is observed for AJAX ONESIDE when applied tension is increased from 25% of T_u to 50% of T_u . Finally, the specimens at 75% T_u did not show any plastic deformation as shown in the load-slip curves. Failure in the linear region is observed for all three steel-

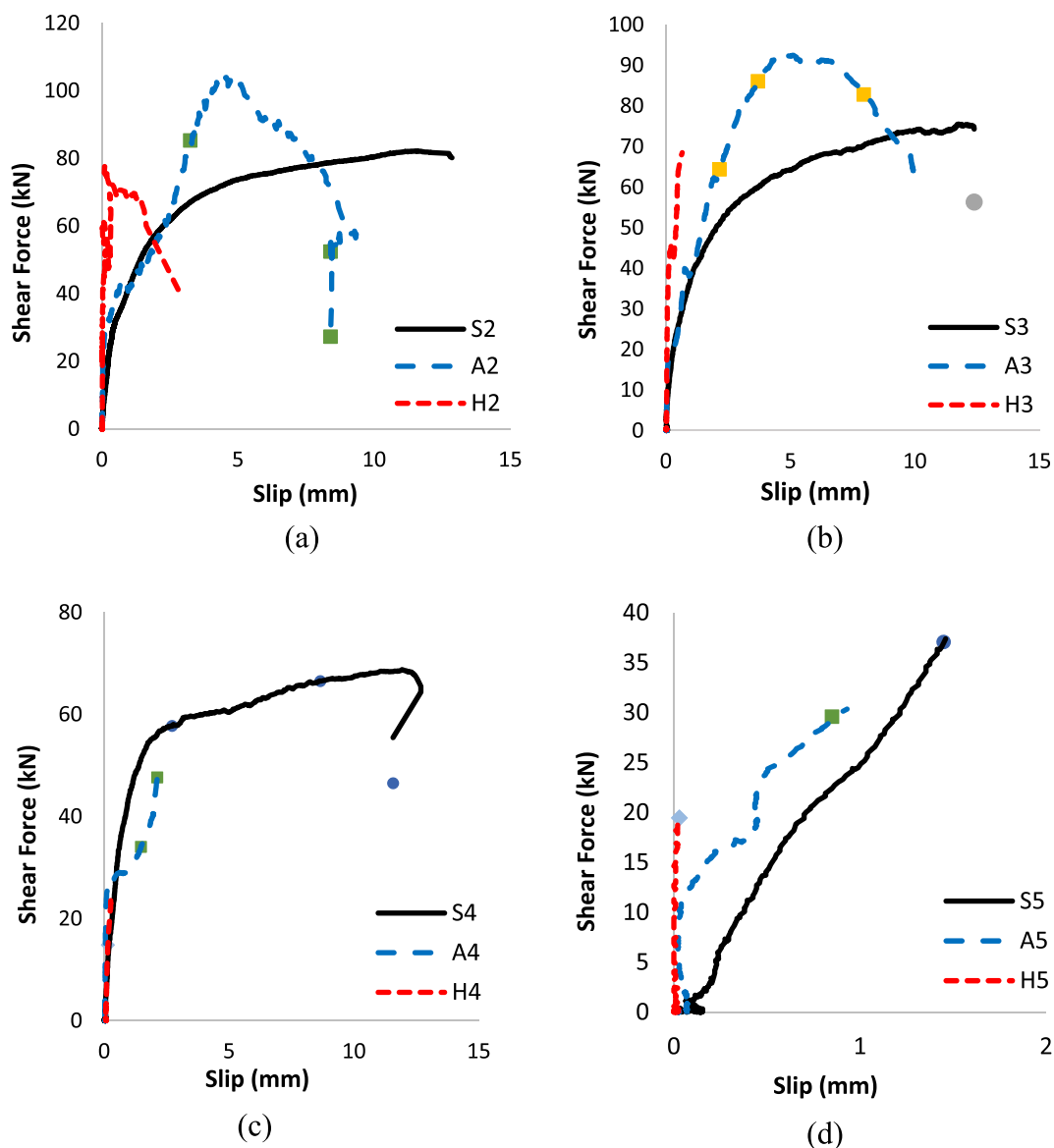


Fig. 10. Load vs slip diagrams, (a) Pure shear loading, (b) At 25% T_u , (c) At 50% T_u , (d) At 75% T_u .

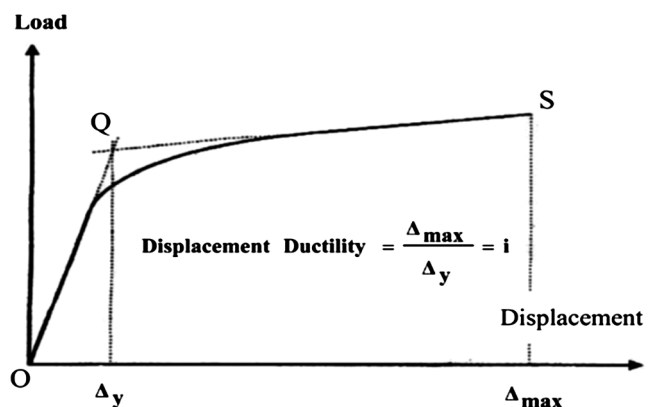


Fig. 11. Ductility index [2].

Table 4
Ductility index for push test and modified push test specimens.

Group	Specimen ID	Δ_y (mm)	Δ_{max} (mm)	i (Eq. (5))
Group 2	S2	1.00	11.05	11.1
	A2	0.60	4.72	7.9
	H2	0.10	1.4	14.0
Group 3	S3	1.00	12.10	12.1
	A3	0.60	4.69	7.2
	H3	0.10	1.20	12
Group 4	S4	0.80	11.92	14.9
	A4	0.20	2.12	10.6
	H4	0.10	0.27	2.7
Group 5	S5	1.46	1.46	1.0
	A5	0.93	0.93	1.6
	H5	0.10	0.10	1.0

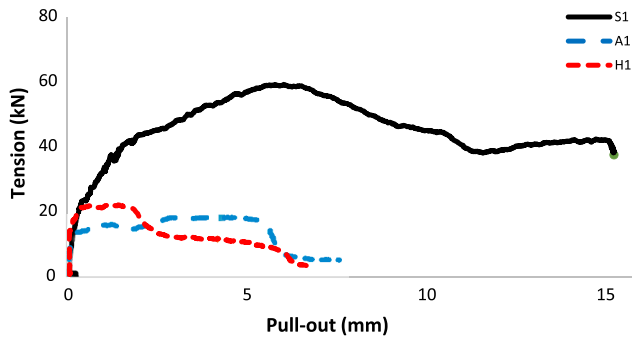


Fig. 12. Load vs pull-out for pure tensile loading.

Table 5
Ductility index for pull out test specimen.

Group	Specimen ID	Δ_y (mm)	Δ_{max} (mm)	i (Eq. (5))
Group 1	S1	1.56	5.70	3.7
	A1	0.2	5.05	25.25
	H1	0.1	1.24	12.4

concrete connector types.

Ductility is the ability of a material to deform permanently in response to tensile stress. The ductility index is that ratio of slip at ultimate load to the slip at yield point, Eq. (5), as shown in Fig. 11 [2,31,32]. From Fig. 11, the intersection of two gradient lines OQ and QS are used to determine the point O to determine the displacement at yield, Δ_y . Gradient line OQ is drawn from the initial gradient of the curve from point O where load is zero. Line QS is drawn from the last gradient of the curve from point S where the load is at maximum.

Fig. 10 is used to determine the ductility index for all three types of steel-concrete connectors. The ductility index values for specimens in Group 2 to 5 are given in Table 4 below. Generally, tension had minimal effect on the ductility index except for specimen H4 and Group 5 specimens which saw a significant reduction in the ductility index. However, it should be noted that a smaller ductility index does not imply the steel-concrete connector is undesirable. This is shown when comparing the ductility index of specimen S2 and H2. In this case, although H2 has a higher ductility index than the ductility index of S2, the headed studs portray desirable behaviour with significant

deformation compared to Holo-Bolts as seen in the load-slip behaviour graph shown in Fig. 10(a).

$$i = \frac{\Delta_{max}}{\Delta_y} \tag{5}$$

4.1.2. Pull out test

The tensile load vs pull-out displacement curve of the three steel-concrete connector types is shown in Fig. 12 below. Both AJAX ONE-SIDE and Holo bolt nearly reach their peak load capacities before any noticeable slip is recorded. The AJAX ONESIDE continues to resist close to peak loads up to a pull-out of around 5 mm after which point breakout occurred and load dropped. For Holo-Bolts, the load gradually decreased after reaching a maximum. On the contrary, demountable headed studs behaved like a typical headed stud under shear load by portraying significant displacement as well as undergoing plastic deformation.

Using Eq. (5), the ductility index of the steel-concrete connectors has been determined when subjected to purely tensile loads. The resulting values of ductility index are given in Table 5. AJAX ONESIDE had the highest ductility with a ductility index of 25.25. However, the failure of AJAX ONESIDE connectors was abrupt and not desirable due to the minimal warning signs before failure. Ideally, the pull-out load of the demountable headed stud would be preferred due to its ability to show significant plastic deformation.

4.2. Failure modes

4.2.1. Pull-out test

Two types of failure modes occurred in the pull-out tests. One of them is concrete breakout due to tension. There are two commonly used methods that estimate the design resistance due to concrete failure and these are the 45° cone failure and the concrete design capacity (CCD) method. In the case of the 45° cone method, the concrete is assumed to form a conical surface around the steel-concrete connector with an angle of approximately 45° as shown in Fig. 13(a) between the concrete member and the concrete failure surface. Based on this method and their test results, Nelson Stud welding [33] recommended an embedment depth that is approximately 8–10 times the shank diameter so that the concrete breakout strength in tension is larger than the tensile failure of the steel-concrete connector material. The second method, CCD, assumes a similar failure mode with the exception being the

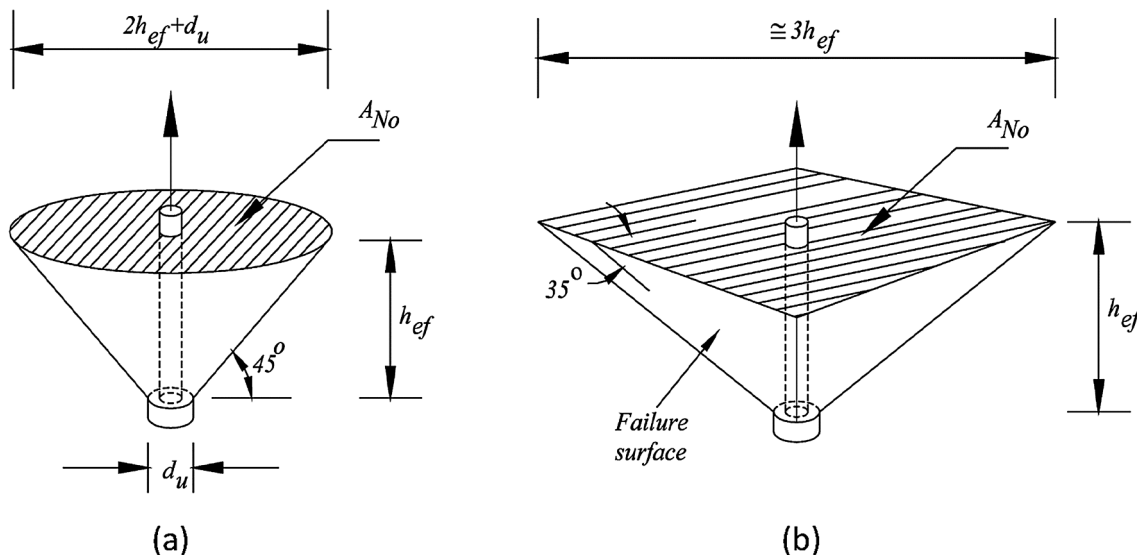


Fig. 13. (a) Conical failure, (b) Four-sided pyramid failure [1].

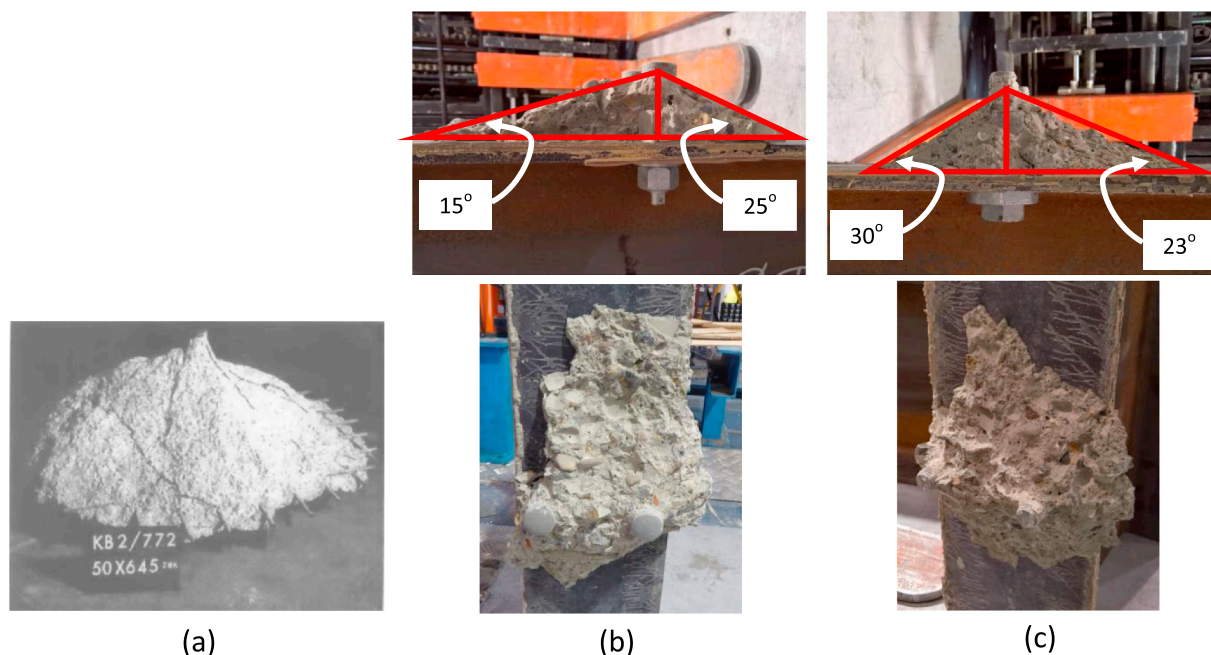


Fig. 14. Failure cones due to tensile loading (a) Headed studs [3], (b) AJAX Oneside, (c) Hollo bolt.



Fig. 15. Concrete splitting failure for specimen S1 (After demounting).

breakout takes the form of a four-sided pyramid with failure angle of 55° between the concrete failure surface and the steel-concrete connector (35° between concrete member and failure surface) as shown in Fig. 13(b). This method makes use of simple equations to estimate the tensile and shear resistance. Various multiplication factors are then used to account for design variations some of which include edge distance and absence of cracking [16]. The CCD method is adopted by ACI 318-14 [26]. Concrete breakout due to tension was observed for specimen A1 and H1 and the failure cones obtained from these specimens are shown in Fig. 14(b) and Fig. 14(c) respectively. The average concrete cone failure angle for the specimens were 20° for the AJAX ONESIDE and 27° for the Hollo Bolt which agrees more with the CCD

method than the 45° cone method. However, the shape of the failure cones was more conical unlike the four-sided pyramid as suggested by the CCD method. The cones obtained were irregular/non-uniform likely due to the material boundaries of aggregate in concrete. Since the headed studs did not undergo concrete breakout, results from Ožbolt et al. [3] been shown in Fig. 14(a) alongside those of AJAX ONESIDE and Hollo-Bolt for comparison purposes.

The second failure mode is splitting failure. This failure mode is also because of concrete failing from tension. However, due to the higher h_{ef}/d_s ratio, the reinforcement was passing through the concrete failure zone. Hence, it kept the concrete intact and prevented the complete separation of the steel beam from the concrete block. Splitting failure was observed for specimen S1 as shown in Fig. 15. Cracks had developed in specimen S1 and the load dropped but the specimen was still intact unlike specimens A1 and H1 which exhibited complete separation at the steel-concrete interface upon failure.

4.2.2. Push tests

Two distinct types of failure modes were observed for the push tests. The first mode being concrete breakout which is because of concrete failing due to crushing resulting in the formation of concrete failure cone. The concrete around the steel-concrete connectors begins to fail from compression before the steel-concrete connector yields resulting in formation of cracks and eventually complete separation of the steel section from the concrete block as shown in Fig. 16.

Both specimen A2 and H2 failed due to concrete breakout. It should be noted that cracking was also observed at the bottom of the concrete block like what has been shown in Fig. 17 indicating edge effects on specimen.

The second failure mode was stud fracture which was observed for specimens S2. In this failure mode, the steel-concrete connector material yields with subsequent and often abrupt fracture of the steel-concrete connector shank. Typically, the shank shears at the steel concrete interface with some cracks emanating from the steel-concrete connectors and concrete crushing visible as shown in Fig. 18.

Two types of failure modes were observed from the combined shear and tensile loading tests. The first mode being concrete breakout which occurred for all specimens involving AJAX ONESIDE and Hollo-bolt.



Fig. 16. Concrete break-out for specimen H2.

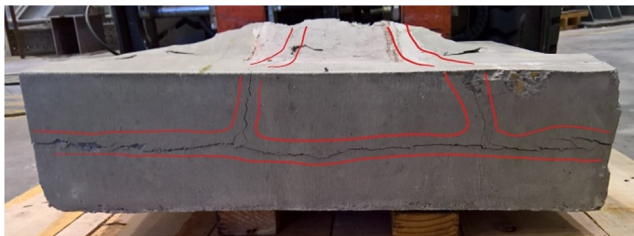


Fig. 17. Cracks in the bottom of the concrete block for A4.

Specimen S5 also failed due to concrete breakout as shown in Fig. 19.

However, the failure was gradual which contrasted with the abrupt failure of the AJAX ONESIDE and Hollo-bolt. S5 was the only demountable headed stud specimen under combine loading to experience concrete breakout. This is because the splitting failure (as observed for specimen S1) inducing tensile load effectively worked in tandem with the shear load to exert higher forces on the concrete and thereby resulting in concrete breakout due to tension. Therefore, the failure occurred at a much lower shear force compared to specimens S2-S4, and hence the demountable headed studs in specimen S5 could resist fracturing. The second failure mode was stud fracture and was observed for specimens S3 and S4.

4.3. Ultimate shear resistance and stiffness

The method to estimate resistance of a steel-concrete connector depends on what failure philosophy is assumed. These philosophies as discussed earlier are the CCD method and the 45° cone method. Various design codes provide formulas to estimate the shear resistance of a steel-concrete connector. Two formulas are generally provided, one for the steel-concrete connector material failure and one for the concrete failure with the lowest value determining the observed failure mode and hence the resistance of that steel-concrete connector. The design expressions of four design codes namely; AS 2327.1 [34], Eurocode 4 [35], PCI 6th [27] and ACI 318-14 [26] are shown Table 6 below.

It should be noted that AS 2327.1 limits the use of its design equations to steel-concrete connectors with an overall height after attachment that is greater than 100 mm. This means the AJAX ONESIDE and Hollo-Bolt do not comply with the requirements of AS 2327.1. However, AS 2327.1 has been used to estimate the resistance of these steel-concrete connector for comparison purposes and to show the need for expressions in AS 2327.1 that can be used in the design process when using stocky steel-concrete connectors.

The test results of Group 2 specimen (pure shear loading) and strength resistance estimates as per the design codes are given in Table 7 below. The ratio of design code estimate against test result is calculated to determine the accuracy of predicting the shear resistance.

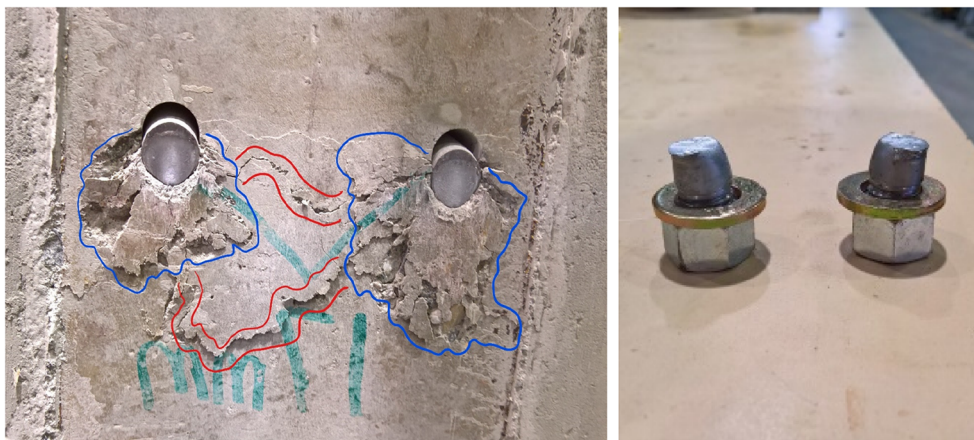


Fig. 18. Stud fracture with concrete crushing for headed studs.



Fig. 19. Significant cracking in specimen S5.

AS 2327.1 predicts the same shear resistance for both AJAX ONESIDE and Hollo-Bolt which was not the case in the test results since height of embedment is not a design parameter in AS 2327.1. It also overestimates the shear resistance of demountable headed studs, AJAX ONESIDE and Hollo-Bolt by 19, 21 and 62% respectively. For AJAX ONESIDE, Eurocode 4 [35] and PCI 6th [27] manage to predict the strength relatively accurately with an estimated resistance that is 2 and 4% lower respectively than the test results. Both Eurocode 4 [35] and PCI 6th [27] overestimate the shear resistance of Hollo-Bolts by 32 and 16% respectively.

Pryout failure is usually the critical failure mode for short and stocky steel-concrete connectors and for this failure mode, the design strength per ACI 318-14 [26] is found by multiplying the respective steel-concrete connector’s tensile resistance due to concrete breakout by a factor k_{cp} . This method results in a significant underestimation of the shear resistance of AJAX ONESIDE and Hollo-Bolts by an approximately 72%.

Table 6
Design expressions for shear resistance.

	AS 2327.1	Eurocode 4	PCI 6th (5% fractile)	ACI 318-14 (5% fractile)
Connector fracture	$0.63d_{bs}^2 f_{uc}$	$0.8A_s f_u$	$A_s f_u$	$A_s f_u$
Concrete failure	$0.31d_{bs}^2 \sqrt{f_{cj} E_c}$ ^a	$0.29\alpha d_{bs}^2 \sqrt{f_{cj} E_c}$ ^a	$215\lambda \sqrt{f_c} d_o^{1.5} h_{ef}^{0.5b}$	$k_{cp} 24\lambda \sqrt{f_c} h_{ef}^{1.5} \psi_{c,N}$ ^b
Units	N, mm	N, mm	pounds, inches	pounds, inches

$$\alpha = 0.2 \left(\frac{h_{sc}}{d} + 1 \right) \text{ for } 3 \leq h_{sc}/d \leq 4.$$

$$\alpha = 1 \text{ for } h_{sc}/d > 4.$$

$$\psi_{c,N} = 1.25 \text{ for cast in anchors.}$$

$$k_{cp} = 1 \text{ for } h_{ef} < 2.5 \text{ in (63.5 mm).}$$

$$k_{cp} = 2 \text{ for } h_{ef} \geq 2.5 \text{ in (63.5 mm).}$$

^a Failure mode not specified.

^b Concrete pry out failure.

Shear stiffness K_{st} , is computed to determine the secant modulus of the load-slip curve up to 50% of V_u . Based on this principle, K_{st} has been calculated and summarised in Table 8. In the design of the test specimens, the clearances between the bolt hole and the bolt rod are kept to the minimum to prevent any slippage at the beginning of the loading phase. For example, a hole diameter of 20 mm will be drilled for a 20 mm diameter bolt. However, from the Table 8, the shear stiffness values for headed studs (S2-5) are low compared to both AJAX ONESIDE (A2-5) and Hollo-Bolts (H2-5). The reason could be due the locking mechanism for AJAX ONESIDE and Hollo-Bolts. Hollo-Bolt has the expanded sleeves as shown in Fig. 4 that slightly reduce any clearance between the hole and bolt rod, whilst AJAX ONESIDE has two interlocked nuts to create additional frictional resistance to prevent slippage at the clearance region. However, the shear stiffness values decrease for all demountable steel-concrete connectors when they are subjected to combined shear and tension.

4.4. Ultimate tensile resistance

Two design codes that provide design guidelines for determining the tensile resistance of steel-concrete connectors are PCI 6th [27] and ACI 318-14 [26] and their respective design expressions are given in Table 9 below.

The test results of Group 1 specimen (pure tensile loading) and the design resistance based on the two design codes are given in Table 10 below. Both PCI 6th [27] and ACI 318-14 [26] overestimate the tensile resistance of AJAX ONESIDE by approximately 44 and 45% respectively whereas for the Hollo-Bolt, they both underestimate tensile resistance by approximately 10%. PCI 6th [27] and ACI 318-14 [26] also overestimate the tensile resistance of demountable headed studs by 32 and 33% respectively. Therefore, PCI 6th [27] and ACI 318-14 [26] are safe to use when designing for Hollo bolts. However, it should not be used when designing for AJAX ONESIDE blind bolts and demountable headed studs.

4.5. Shear and tension interaction resistance

The test results for the shear resistance of steel-concrete connectors under combined loading are summarised in Table 11. The interaction diagrams for the demountable head studs, AJAX ONESIDE and Hollo Bolts are plotted in Fig. 20. As shown in the graphs, there is a significant decrease in shear strength depending on the tension being applied. For headed studs, the shear resistance reduced by approximately 7, 19 and 56% when the tensile resistance was increased by 25, 50 and 75% respectively. For AJAX ONESIDE, the shear resistance reduced by 11, 54 and 71% when the tensile resistance was increased by 25, 50 and 75% respectively. For Hollo-Bolts, the shear resistance reduction of 12, 68 and 75% was observed when the tensile resistance was increased by 25, 50 and 75% respectively.

Table 7
Push test results.

Group	Specimen ID	V_u (kN)	AS 2327.1 (kN)	EC 4 (kN)	PCI 6th (kN)	ACI 318-08 (kN)	$\frac{AS}{Test}$	$\frac{EC4}{Test}$	$\frac{PCI}{Test}$	$\frac{ACI}{Test}$	s_u (mm)	Failure mode
2	S2	84.8	100.7 ^a	100.4 ^a	125.5 ^a	125.5 ^a	1.19	1.18	1.48	1.48	11.05	Stud fracture
	A2	104.3	126.7 ^b	101.9 ^b	99.7 ^b	28.9 ^b	1.21	0.98	0.96	0.28	4.72	Concrete breakout
	H2	78.0	126.7 ^b	103.1 ^b	90.3 ^b	21.5 ^b	1.62	1.32	1.16	0.28	0.11	Concrete breakout

^a Connector fracture.^b Concrete failure.**Table 8**
Shear stiffness for push test and modified push test specimens.

Group	Specimen ID	K_{si} (kN/mm)
Group 2	S2	69
	A2	1600
	H2	1920
Group 3	S3	67
	A3	562
	H3	750
Group 4	S4	67
	A4	500
	H4	166
Group 5	S5	27
	A5	132
	H5	677

Table 9
Design expressions for tensile resistance.

	PCI 6th (5% fractile)	ACI 318-14 (5% fractile)
Connector fracture	$A_s f_u$	$A_s f_u$
Concrete failure (breakout)	$3.33\lambda \sqrt{\frac{f_c}{h_{ef}}} (9h_{ef}^2)$	$24\lambda \sqrt{f_c} h_{ef}^{1.5} \psi_{c,N}$
Units	Pounds, inches	Pounds, inches

Headed studs show an elliptical relationship between the tensile resistance and the shear resistance whereas AJAX ONESIDE connectors and Hollo-Bolts had a relatively linear relationship. The square of the Pearson product moment correlation coefficient (R^2) was calculated to assess the fit of the test data to the relationships proposed by McMackin et al. [23], Bode et al. [24,25], and Lin et al. [14]. R^2 is a value calculated by spreadsheet programs to determine how well a range of data fits a trend line. The closer the R^2 value is to 1, the more accurate the equation estimates the data. If the R^2 value is 0, there is no relationship between the data. Table 12 shows the calculated R^2 value for three equations for all three steel-concrete connector types.

For headed studs, the three relationships Eqs. (1)–(3) closely predict the test data. Eq. (3) has the highest accuracy with an R^2 value of 0.9887. For AJAX ONESIDE connectors, both Eqs. (1) and (3) overestimate the resistance with R^2 values of 0.8522 and 0.8786 respectively. Eq. (2) manages to closely predict the interaction with an R^2 value of 0.9347. However, based on the test results, a perfectly linear relationship accurately predicts the resistance with an R^2 value of

0.9655. For Hollo-Bolt connectors, Eqs. (1)–(3) overestimate the resistance considerably with R^2 values of 0.7575, 0.7883 and 0.8600 respectively. Based on the test results, a perfectly linear relationship can predict the resistance relatively accurately under combined loading with an R^2 value of 0.9363.

5. Conclusion

Tests were carried out on a total of fifteen specimens for three types of steel-concrete connectors subjected to shear, tensile and combined shear and tensile loading. Upon analysis of the results and comparison with existing design codes and interaction relationships, the following conclusions were drawn:

- (1) Demountable headed studs are ductile as shown by the significant slip demonstrated in its load-slip behaviour when under pure shear loading compared to AJAX ONESIDE and Hollo bolts. However, this increased ductility is not shown when calculating the ductility index which relies solely on the slip at yield point and at ultimate load.
- (2) Significant reduction in shear resistance was observed when tensile force was applied. Hollo bolts had the highest percentage reduction in shear resistance whereas demountable headed studs had the lowest reduction in shear resistance for specimens in each group.
- (3) The primary mode of failure for demountable headed studs was stud fracture whereas for AJAX ONESIDE and Hollo-Bolts, it was concrete breakout owing to the high material strength of AJAX ONESIDE and Hollo bolts.
- (4) AJAX ONESIDE had the highest ultimate shear resistance (104.3 kN) of the three whereas demountable headed studs had the highest ultimate tensile resistance of the three (60 kN).
- (5) Hollo-Bolts achieved the highest shear stiffness due their locking mechanism using their expanded sleeves. However, the shear stiffness decreased in the presence of tension for all steel-concrete connectors.
- (6) The design codes give varying accuracies when predicting the ultimate shear resistance and ultimate tensile capacities. The largest difference between the strength resistance based on design codes and test results was when using ACI 318-14 [26] to predict shear resistance of AJAX ONESIDE and Hollo-Bolts.
- (7) All three types of steel-concrete connectors followed different interaction relationships. Demountable headed studs had an elliptical relationship compared to the linear relationship observed for AJAX ONESIDE and Hollo bolts.

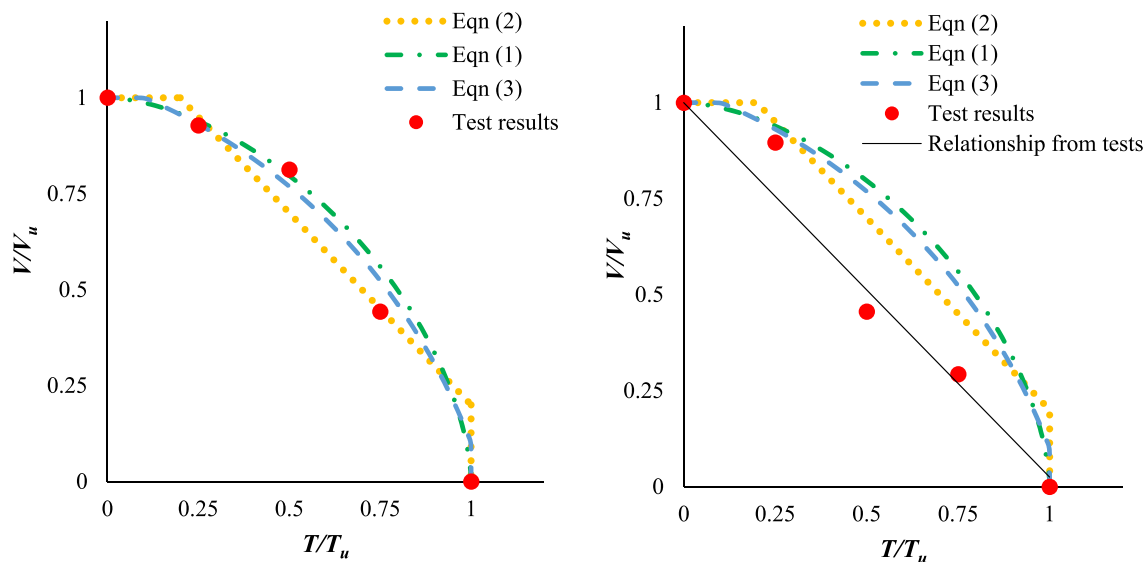
Table 10
Pull-out test results.

Group	Specimen ID	T_u (kN)	PCI 6th (kN)	ACI 318-14 (kN)	$\frac{PCI}{Test}$	$\frac{ACI}{Test}$	Maximum vertical pull-out (mm)	Failure mode
1	S1	60	79.4 ^a	79.5 ^a	1.32	1.33	5.70	Concrete splitting
	A1	20	28.8 ^b	28.9 ^b	1.44	1.45	5.4	Concrete breakout
	H1	24	21.5 ^b	21.5 ^b	0.90	0.90	1.24	Concrete breakout

^a Connector fracture.^b Concrete failure.

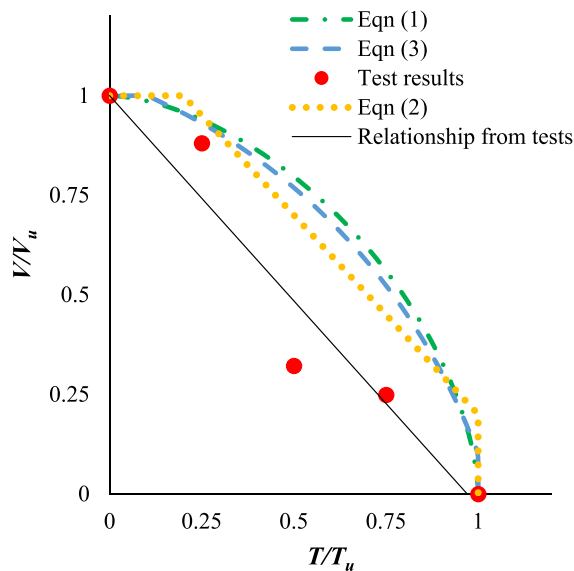
Table 11
Push test and modified push test results.

Group	Specimen ID	% of T_u applied	T_{cu} (kN)	V_u (kN)	V_{cu} (kN)	Shear resistance reduction (%)	Failure mode
2	S2	–	–	84.8	–	–	Stud fracture
	A2	–	–	104.3	–	–	Concrete breakout
	H2	–	–	78.0	–	–	Concrete breakout
3	S3	25	15	–	78.5	7.4	Stud fracture
	A3	25	5	–	93.3	10.5	Concrete breakout
	H3	25	6	–	68.8	11.8	Concrete breakout due to tension
4	S4	50	30	–	68.8	18.9	Stud fracture
	A4	50	10	–	47.5	54.4	Concrete breakout due to tension
	H4	50	12	–	25.0	67.9	Concrete breakout due to tension
5	S5	75	45	–	37.5	55.8	Concrete breakout due to tension
	A5	75	15	–	30.5	70.8	Concrete breakout due to tension
	H5	75	18	–	19.5	75.0	Concrete breakout due to tension



(a) Demountable headed stud

(b) AJAX ONESIDE



(c) Hollo-Bolt

Fig. 20. Comparison of test results with existing relationships for shear-tension interaction.

Table 12
R² value comparison.

	Calculated R ²		
	Headed Stud	AJAX ONESIDE	Hollo-Bolt
Eq. (1)	0.9834	0.8522	0.7575
Eq. (2)	0.9828	0.9347	0.8600
Eq. (3)	0.9887	0.8786	0.7883
Linear relationship	–	0.9655	0.9363

(8) Due to the low ultimate tensile resistance for both AJAX ONESIDE and Hollo bolts, they are not suitable in the application of composite walls where they could be subjected combined tensile and shear loads. However, they are suitable for composite beams where they are only subjected to high shear loads.

Acknowledgments

The experimental testing was funded by 2016 RIF Challenge Project Funding from the School of Computing, Engineering and Mathematics of Western Sydney University. The authors would also like to thank the technical staffs of the Structures Laboratory at Western Sydney University for their assistance with the experimental testing.

Appendix A. Supplementary material

Supplementary data to this article can be found online at <https://doi.org/10.1016/j.engstruct.2018.12.088>.

References

- [1] Ashour A, Alqedra M. Concrete breakout strength of single anchors in tension using neural networks. *Adv Eng Softw* 2005;36(2):87–97.
- [2] Rakhshanimehr M, Esfahani MR, Kianoush MR, Mohammadzadeh BA, Mousavi SR. Flexural ductility of reinforced concrete beams with lap-spliced bars. *Can J Civ Eng* 2014;41(7):594–604.
- [3] Özbolt J, Elighausen R, Reinhardt HW. Size effect on the concrete cone pull-out load. *Int J Fract* 1999;95(1):391.
- [4] Oehlers DJ, Coughlan CG. The shear stiffness of stud shear connections in composite beams. *J Constr Steel Res* 1986;6(4):273–84.
- [5] Ollgaard J, Slutter R, Fisher J. Shear strength of stud connectors in lightweight and normal weight concrete. *AISC Eng'g Jr* 1971;71-10(April).
- [6] Shim C-S, Lee P-G, Yoon T-Y. Static behavior of large stud steel-concrete connectors. *Eng Struct* 2004;26(12):1853–60.
- [7] Shen MH, Chung KF. Structural behaviour of stud shear connections with solid and composite slabs under co-existing shear and tension forces. *Structures* 2016.
- [8] Yang F, Liu Y, Jiang Z, Xin H. Shear performance of a novel demountable steel-concrete bolted connector under static push-out tests. *Eng Struct* 2018;160:133–46.
- [9] Kwon G, Engelhardt MD, Klingner RE. Behavior of post-installed shear connectors under static and fatigue loading. *J Constr Steel Res* 2010;66(4):532–41.
- [10] Kwon G, Engelhardt MD, Klingner RE. Experimental behavior of bridge beams retrofitted with postinstalled shear connectors. *J Bridge Eng* 2011;16(4):536–45.
- [11] Liu X, Bradford MA, Lee MSS. Behavior of high-strength friction-grip bolted shear connectors in sustainable composite beams. *J Struct Eng* 2014;141(6):04014149.
- [12] Suwaed ASH, Karavasilis TL. Novel demountable shear connector for accelerated disassembly, repair, or replacement of precast steel-concrete composite bridges. *J Bridge Eng* 2017;22(9):04017052.
- [13] Saari WK, Hajjar JF, Schultz AE, Shield CK. Behavior of shear studs in steel frames with reinforced concrete infill walls. *J Constr Steel Res* 2004;60(10):1453–80.
- [14] Lin Z, Liu Y, He J. Behaviour of stud connectors under combined shear and tension loads. *Eng Struct* 2014;81(1):362–76.
- [15] Mirza O, Uy B. Effects of the combination of axial and shear loading on the behaviour of headed stud steel anchors. *Eng Struct* 2010;32(1):93–105.
- [16] Pallarés L, Hajjar JF. Headed steel stud anchors in composite structures, Part II: Tension and interaction. *J Constr Steel Res* 2010;66(2):213–28.
- [17] Henderson IEJ, Zhu XQ, Uy B, Mirza O. Dynamic behaviour of steel–concrete composite beams with different types of steel-concrete connectors. Part I: experimental study. *Eng Struct* 2015;103:298–307.
- [18] Moynihan MC, Allwood MJ. Viability and performance of demountable composite connectors. *J Constr Steel Res* 2014;99(1):47–56.
- [19] Pavlović M, Marković Z, Veljković M, Buđevac D. Bolted steel-concrete connectors vs. headed studs behaviour in push-out tests. *J Constr Steel Res* 2013;88:134–49.
- [20] Rehman N, Lam D, Dai X, Ashour AF. Experimental study on demountable steel-concrete connectors in composite slabs with profiled decking. *J Constr Steel Res* 2016;122(1):178–89.
- [21] Lee S-SM, Bradford MA. Sustainable composite beam behaviour with deconstructable bolted steel-concrete connectors. *Proceedings of the Composite Construction VII, Palm, Cove, Queensland: Australia; 2013.*
- [22] Dai XH, Lam D, Saveri E. Effect of concrete strength and stud collar size to shear capacity of demountable steel-concrete connectors. *J Struct Eng* 2015;141(11). article number 04015025.
- [23] McMackin PJ, Slutter RG, Fisher JW. Headed steel anchors under combined loading. *AISC Eng J* 1973;10(2):43–52.
- [24] Bode H, Hanenkamp W. Strength of headed bolts subjected to tensile Loads. *Bauingenieur Berlin* 1985;60(9):361–7.
- [25] Bode H, Roik K. Headed studs-embedded in concrete and loaded in tension. *Spec Publ* 1987;103.
- [26] American Concrete Institute. *ACI 318-14: Building Code Requirements for Structural Concrete and Commentary*, Farmington Hills; 2014.
- [27] *PCI design handbook. Precast and Prestressed Concrete*. 6th ed. Chicago: Precast/Prestressed Institute; 2005.
- [28] Standards Australia Online, 2014, AS1012.9:2014, Methods of testing concrete - Compressive strength tests - Concrete, mortar and grout specimens, SAI Global database.
- [29] Standards Australia Online, 1997, AS1012.17-1997, Methods of testing concrete - Determination of the static chord modulus of elasticity and Poisson's ratio of concrete specimens, SAI Global database.
- [30] Standards Australia Online, 2000, AS1012.11:2000, Methods of testing concrete - Determination of the modulus of rupture, SAI Global database.
- [31] Azizinamini A, Pavel R, Hatfield E, Ghosh S. Behavior of lap-spliced reinforcing bars embedded in high-strength concrete. *Struct J* 1999;96(5):826–35.
- [32] Cohn M, Bartlett M. Computer-simulated flexural tests of partially prestressed concrete sections. *J Struct Div* 1982;108(12):2747–65.
- [33] Welding NS. Embedment properties of headed studs, Design data 10. Lorain, OH: Nelson Division; 1974.
- [34] Standards Australia Online, 2003, AS2327.1-2003, Composite Structures Part 1: Simply supported beams, SAI Global database.
- [35] European Committee for Standardization, 1994, Eurocode 4: design of composite steel and concrete structures.